

**TEMPERATURE BEHAVIOR IN THE BUILD SECTION  
OF MULTILATERAL WELLS**

A Thesis

by

ANALIS ROMERO LUGO

Submitted to the Office of Graduate Studies of  
Texas A&M University  
in partial fulfillment of the requirements for the degree of  
MASTER OF SCIENCE

August 2005

Major Subject: Petroleum Engineering

**TEMPERATURE BEHAVIOR IN THE BUILD SECTION  
OF MULTILATERAL WELLS**

A Thesis

by

ANALIS ROMERO LUGO

Submitted to the Office of Graduate Studies of  
Texas A&M University  
in partial fulfillment of the requirements for the degree of  
**MASTER OF SCIENCE**

Approved by:

Chair of Committee, A. Daniel Hill

Committee Members, Ding Zhu

J. Eric Bickel

Head of Department, Steve Holditch

August 2005

Major Subject: Petroleum Engineering

## ABSTRACT

Temperature Behavior in the Build Section of Multilateral Wells. (August 2005)

Analís Romero Lugo, B.S., Universidad del Zulia

Chair of Advisory Committee: Dr. A. Daniel Hill

Intelligent well completions are increasingly being used in horizontal, multilateral, and multi-branching wells. Such completions are equipped with permanent sensors to measure temperature and pressure profiles, which must then be interpreted to determine the inflow profiles of the various phases produced that are needed to characterize the well's performance. Distributed temperature measurements, using fiber optics in particular, are becoming increasingly more often applied.

The value of an intelligent completion hinges on our capability to extract such inflow profiles or, at a minimum, to locate the entry locations of undesirable water or gas entries.

In this research, a model of temperature behavior in multilateral wells was developed. The model predicts the temperature profiles in the build sections connecting the laterals to one another or to a main wellbore, thus accounting for the changing well angle relative to the temperature profile in the earth. In addition, energy balance equations applied at each junction predict the effects of mixing on the temperature above each junction.

The multilateral wellbore temperature model was applied to a wide range of cases, in order to determine the conditions for which intelligent completions would be most useful. Parameters that were varied for this experiment included fluid thermal properties, absolute values of temperature and pressure, geothermal gradients, flow rates from each

lateral, and the trajectories of each build section. From this parametric study, guidelines for an optimal application of intelligent well completion are represented.

## DEDICATION

I wish to dedicate my thesis first to God, who has been my guide in life I thank you,  
Father, for so many blessings;

To my parents, Jose Domingo, and Nancy for their support, encouragement, sacrifices,  
and especially for their unconditional love, I love you both;

To my sisters and brother, Anabella, Ana Carola, and Jose Domingo for their help,  
caring and the great moments we spent together. I love you too.

## ACKNOWLEDGMENTS

I wish to express my sincere gratitude and appreciation to Dr. A. Daniel Hill, chair of my advisory committee, for his enthusiastic and active participation and guidance throughout my research; and Dr. Ding Zhu, member of my advisory committee, for her continued help and support throughout my project. It was an honor to work with her.

I also I want to thank Dr. J. Eric Bickel, member of my advisory committee, for his help in completing this project; and Dr. Larry Lake, member of research group, for his wise words and his unconditional support and advice. Thank you so much.

I am grateful to the Department of Energy (DOE), sponsors of this research, for their financial support of this project.

Finally, I want to express my gratefulness to and admiration of all my colleagues at Texas A&M University and The University of Texas at Austin, especially to Keita Yoshioka and Pinan Dawkrajai.

## TABLE OF CONTENTS

	Page
ABSTRACT.....	iii
DEDICATION.....	v
ACKNOWLEDGMENTS.....	vi
TABLE OF CONTENTS .....	vii
LIST OF FIGURES.....	ix
LIST OF TABLES.....	x
CHAPTER	
I INTRODUCTION.....	1
1.1 Background and Purpose of Research .....	1
1.2 Objectives .....	2
1.3 Problem Description .....	2
1.4 Motivation: Wells of the Future .....	3
II LITERATURE REVIEW.....	4
2.1 Previous Models .....	4
III FUNDAMENTALS .....	9
3.1 Model Description .....	9
3.2 Build Section .....	9
3.3 Junction Mixing Model.....	10
IV SENSITIVITIES STUDIES AND RESULTS.....	12
4.1 Temperature Profiles along the Build Section with Different Trajectories	12
4.2 Temperature Profiles for Multilaterals: Dual-Lateral with Single-Phase Liquid.....	15
4.3 Cases with Different Fractions of Total Production from Each Lateral: Dual-Lateral with Single-Phase Liquid .....	19
4.4 Temperature Profiles for Multilaterals: Dual-Lateral with Single-Phase Gas.....	26
4.5 Summary.....	28
V CONCLUSIONS.....	30

	Page
NOMENCLATURE.....	31
REFERENCES.....	33
APPENDIX A.....	35
APPENDIX B.....	42
VITA.....	47



## LIST OF FIGURES

FIGURE	Page
2.1 Transient heat conduction in an infinite radial system.....	5
4.1 Temperature profiles along the build section (3000 STB/D).....	13
4.2 Constant radius of curvature and constant angle trajectory .....	14
4.3 Temperature profiles along the build section (200 STB/D).....	15
4.4 Dual lateral geometry for examples .....	16
4.5 Build section temperature profiles with liquid production at the same depth.....	17
4.6 Build section temperature profiles with liquid production at depths spaced 500 feet apart.....	18
4.7 Build section temperature profiles with liquid production at depths spaced 1000 feet apart.....	18
4.8 Build section temperature profiles with different rates of 3000 STB/D and 500 STB/D .....	19
4.9 Fraction of total production from each lateral: 20% - 80%.....	21
4.10 Fraction of total production from each lateral: 30% - 70%.....	21
4.11 Fraction of total production from each lateral: 40% - 60%.....	22
4.12 Fraction of total production from each lateral: 50% - 50%.....	23
4.13 Fraction of total production from each lateral: 60% - 40%.....	24
4.14 Fraction of total production from each lateral: 70% - 30%.....	25
4.15 Fraction of total production from each lateral: 80% - 20%.....	25
4.16 Build section temperature profiles with gas production at the same depth.....	27
4.17 Build section temperature profiles with gas production at depths spaced 500 feet apart .....	27
4.18 Build section temperature profiles with gas production at depths spaced 1000 feet apart .....	28

**LIST OF TABLES**

TABLE	Page
4.1 Main Characteristics of the Reservoir-Build Section with Different Trajectories	13
4.2 Main Characteristics of the Reservoir - Temperature Profiles for Multilaterals: Dual-Lateral with Single-Phase Liquid .....	17
4.3 Main Characteristics of the Reservoir - Temperature Profiles for Multilaterals: Dual-Lateral with Single-Phase Gas .....	26

## CHAPTER I

### INTRODUCTION

#### 1.1 Background and Purpose of Research

Well monitoring, surveillance, and problem diagnosis are all important parts of the production business, and many production parameters are monitored during this process. Of these, flow rate and fluid type (phase) are two of the most fundamental of the accumulated measurements. Over the years, many instruments have been used to collect and process flow data, including production logging tools, surface test separators, and surface multiphase flow-meters, but none of these provide a complete information solution. Production logs provide flow information as a function of depth, but only intermittently over time. In addition, production logging tools are complicated, especially those designed for deviations beyond 45° from vertical, which is the case in a multilateral well. The traditional method of flow analysis relies on routine periodic production testing through a separator, and back allocation of production over the intervals between tests. Restricted access to a test separator often imposes constraints on when this information can be gathered. The empirical relationships used to estimate the rates between valid tests are often vulnerable to those errors and uncertainties associated with varying flow conditions and data limitations. Permanent downhole sensors are the solution to all these problems. They are used to measure temperature and pressure profiles, are reliable and simple, can be operated at any deviation angle, and are capable of real-time response. Distributed temperature measurements using fiber optics, in particular, are becoming increasingly applied. The value of an intelligently completed design hinges on our capability to extract such inflow profiles or, at a minimum, to identify the entry locations of undesirable water or gas entries.

---

This thesis follows the style of the *SPE Reservoir Evaluation and Engineering Journal*.

## 1.2 Objectives

The main objective of this thesis is to predict temperature profiles in the build sections connecting the laterals to one another or to a main wellbore, thus accounting for the changing well angle relative to the temperature profile in the earth. In addition, energy balance equations applied at each junction will predict the effects of mixing on the temperature above each junction.

The results of this work will allow researches to have a better idea of the effects of those parameters such as fluid thermal properties, geothermal gradients, flow rates from each lateral, and the trajectories of each build section have in absolute temperatures. In the case of modeling the wellbore junctions and having commingled fluids with different properties, the mixing method<sup>1</sup> was first reviewed. According to this method, an enthalpy balance is applied to the mixing of two streams of fluid at different temperatures into one combined stream, in order to determine the relative flow rates of those streams.

## 1.3 Problem Description

The build section can be defined as a section of wellbore that is closed to the formation and that connects the productive lateral to the main wellbore or to another lateral. The temperature and pressure profiles of these build sections are needed to relate the temperature and the pressure at the junction locations to the temperatures and pressures of the source laterals.

Sensitivity studies for both single phase liquid and single phase gas are presented in this work where the temperature at the junction is considered to be a function of the flow rates from each lateral, as well as the distance between the laterals, the fluid thermal properties, and the geothermal gradient. In the plots used to analyze those effects, lines with a maximum value were observed when lateral 1 had a higher flow rate than lateral 2, and lines with a minimum value were observed when lateral 2 had a higher flow rate

than lateral 1, which made it easy to distinguish what variables have more significant effects than others.

#### **1.4 Motivation: Wells of the Future**

The motivation for this study is the belief that intelligent completions, specifically those with distributed temperature sensors, will be the future tool in improving well performance. These tools allow rapid reaction in the case of gas or water breakthrough by allowing a quick shutting in of the control valve of a lateral as well as improving the control and production measurements by not forcing engineers to wait for production tests to identify problems in the well. These intelligent completions will also maximize ultimate recovery, minimize operating expenditures by reducing the number of visits from the operator to the field, reduce well intervention costs, and accelerate production by increasing the contact area between the wellbore and the reservoir. A model of temperature behavior will help operators to understand and utilize intelligent completion more efficiently.

## CHAPTER II

### LITERATURE REVIEW

#### 2.1 Previous Models

During the past few years, several authors have studied practical methods for the calculation of temperatures in the wellbore, understanding that there is transmission of heat between the fluids and the earth as a result of the variation between the fluid and geothermal temperature. In order to develop a model to determine the temperature profile of build sections, several works to predict this temperature profile in a flowing well were studied.

Ramey<sup>2</sup> established a solution for the temperature distribution through the wellbore for injection and production wells of either a single-phase incompressible liquid, or a single-phase ideal gas, taking into consideration that heat transmission in the wellbore was similar to heat flow in the formation. Also, the physical and thermal properties of the earth and wellbore were assumed to be constant with the temperature resulting in a steady-state solution. Solutions for radial heat conduction from an infinitely long cylinder were presented by Carslaw and Jaeger<sup>3</sup> to estimate the time function for a cylinder losing heat at a constant temperature, a constant heat-flux line source, and a loss of heat under the radiation or convection boundary condition. Figure 2.1 shows that all solutions, in the end, come together to form the same line. In earlier stages this solution could generate significant errors, but for long times of greater duration, the line source can be expressed by, the following equation:

$$f(t) = -\ln \frac{r_2}{2\sqrt{\alpha t}} - 0.29 + \frac{r_2^2}{4\alpha t} \dots\dots\dots(2.1)$$

Parameters such as overall heat transfer has been calculated accounting for all the resistances to heat flow presented by the fluid inside the tubing, the tubing wall, fluids or solids in the annulus, and the casing wall. However, some assumptions made to calculate this variable are as follows:

1. Due to the higher thermal conductivity of steel, the thermal resistance of the pipe is neglected.
2. The thermal resistance from liquid water or condensing steam can be ignored because of the high value of the corresponding heat transfer film coefficients.
3. The resistance of cement must be considered because of its low conductivity.

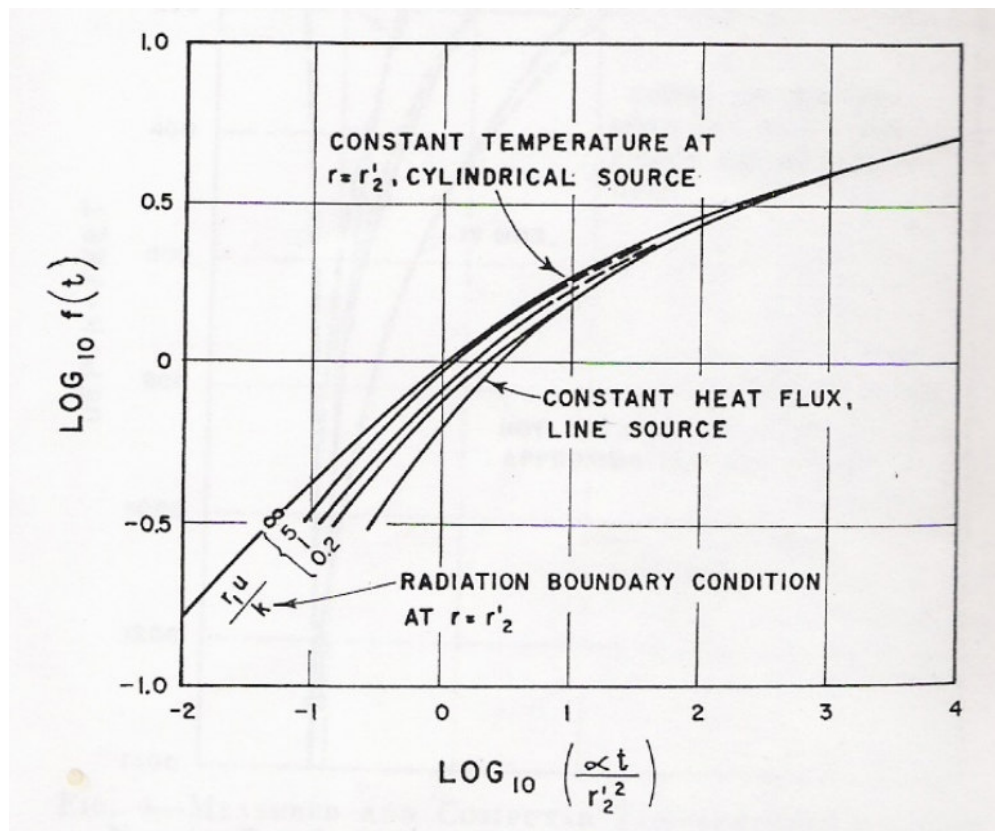


**Fig. 2.1- Transient heat conduction in an infinite radial system<sup>3</sup>.**

Chen<sup>4</sup> developed a model to predict the performance of multilateral wells which calculates the production of each lateral that couples the reservoir inflow model to the wellbore model. Also, the pressure drop in the horizontal lateral was taken into account in this model. Then, the horizontal lateral model was incorporated into a well system with more than one lateral commingled to the main wellbore. As a result of the production of each lateral, the overall production rate and the pressure in the well system can be predicted by the multilateral deliverability model. Single phase and two phase wellbore models were used for flow in the laterals. The single phase lateral flow model includes accelerational and frictional pressure drops, and the two phase lateral flow model applies the Beggs-Brill correlation (or Ouyang's homogeneous model) which accounts for the consequences of the wall inflow, acceleration, and flow patterns. The pressure drop in the tubing from the upper most lateral to the surface was determined using a two phase flow correlation.

Two models were used before this new model for calculating the horizontal laterals:

1. The steady state model using a potential fluid flow was proposed by Joshi<sup>5</sup> which, in general, underestimates productivity.
2. The straightforward model to calculate productivity at a constant flowing bottomhole pressure or a constant rate from a bounded reservoir was presented by Babu and Odeh<sup>6</sup>.

Sagar<sup>7</sup> derived a model to predict temperature profiles in two-phase flowing wells based on the steady state energy equation, which allows for the heat transfer mechanisms found in a wellbore. It was developed with measured temperature data from 392 vertical wells, accounting for kinetic energy effects and Joule-Thomson expansion.

The correlation developed by multiple regression analysis is a function of known physical properties (independent variables) specific to a length interval. The correlation should be used for rates less than 5.0 lbm/sec based on the fact that Joule-Thomson and kinetic energy effects would tend to be less when a smaller amount of gas is present, so



for higher flow rates than that, the value of the result is very close to zero. Also, the radial well dimensions and oil fractions do not contribute to the Joule-Thomson and kinetic energy effects.

$$\begin{aligned} \bar{F}_c = & -2.978 \times 10^{-3} + 1.006 \times 10^{-6} pwh + 1.906 \times 10^{-4} wt - 1.047 \times 10^{-6} R_{gL} + 3.229 \times 10^{-5} \gamma_{API} + \\ & + 4.009 \times 10^{-3} \gamma_g - 0.3551 g_G \dots\dots\dots(2.2) \end{aligned}$$

The Joule-Thomson coefficient states that the quantity of heating or cooling is due to pressure changes within a fluid flowing up the well. Joule-Thomson cooling would normally take place in certain gas-condensate systems and could be determined from the mixture composition. Also, it is usually associated with a higher gas component in the two phase mixture. Joule-Thomson heating is present in wells having comparatively high liquid holdups attributable to either lower gas/liquid ratios or higher wellhead pressures. Another term that tends to be relatively small except for high gas/liquid ratios and low wellhead pressures is kinetic energy.

In addition, several benefits were found by the above listed authors in predicting temperature distribution for two phase flows:

1. The design of production facilities would be improved.
2. Calculations for the two phase flow pressure drop predictions would be more exact.
3. The prediction of temperatures at valve depth would improve gas lift design, improving the predictability of valve throughput.

Hasan and Kabir,<sup>8,9</sup> as well as many other authors, have established that the temperature of the fluid in the wellbore depends upon of the rate of heat loss from the wellbore to the formation, depth and time.

The model determines temperatures in the wellbore through steady state two phase conditions, including a new solution for the thermal diffusivity equation and the consequence of both conductive and convective heat transport for the wellbore system and formation. Then the model shows that as free gas increases, the temperature at the wellhead decreases due to the Joule-Thomson cooling effect.

To determine the formation temperature at distribution, the initial formation temperature was assumed to stay time-invariant, and the outer boundary formation temperature would not to be modified by radial distance.

This model permits conduction and convection for the fluid in the tubing-casing annulus to calculate the overall heat transfer. In the past, convection was not taken into account the resulting high temperature of the fluid.

## CHAPTER III

### FUNDAMENTALS

#### 3.1 Model Description

We have formulated two models to describe the temperature profiles along the variable inclination build sections of multilateral wells, and to describe the resulting temperature when two fluid streams are mixed at a multilateral well junction. To model the temperature profile in a build section, we adapted Ramey's<sup>2</sup> method to the variable inclination geometry of the build section, assuming a constant radius of curvature between the horizontal wellbore and the main wellbore. Other trajectories can be handled in a manner similar to that presented here. To determine the temperature of the mixed stream just above the junction, we applied an enthalpy balance to two streams commingled at the junction.

#### 3.2 Build Section

The equations describing temperature along the build section for single-phase liquid and gas are described in Appendix A. The expression for single-phase liquid for the first build segment is:

$$T_f = T_{Gibh} - g_G \sin \alpha \left[ (L-z) - \left( 1 - \exp\left(\frac{(z-L)}{A}\right) \right) A \right] \dots\dots\dots(3.1)$$

And for any other segment is:

$$T_f = T_{Gi} + Ag_G \sin \alpha + \{T_{f\ known} - T_{Gi} - Ag_G \sin \alpha\} \exp[(z-L)/A] \dots\dots\dots(3.2)$$

Correspondingly, the expression for single-phase gas for the first build segment is:

$$T_f = T_{Gibh} + \left\{ A - A \left[ \exp((z-L)/A) \right] \right\} \left( g_G \sin \alpha - \frac{g \sin \alpha}{C_p J g_c} \right) \dots \dots \dots (3.3)$$

And, for any other segment is:

$$T_f = T_{Gi} + A \left( g_G \sin \alpha - \frac{g \sin \alpha}{C_p J g_c} \right) + \exp[(z-L)/A] \left\{ T_{f \text{ known}} - T_{Gi} + A \left( g_G \sin \alpha - \frac{g \sin \alpha}{C_p J g_c} \right) \right\} \dots (3.4)$$

We approximated the trajectory of a build section with a constant radius of curvature by a number of discrete wellbore increments, each having a constant angle described in Appendix B. The temperature profile was developed beginning with the lowest segment, which is connected to a horizontal lateral of known temperature. Moving up the build section, each lateral segment's temperature was based on the temperature of the previous segment.

### 3.3 Junction Mixing Model

For the case of modeling the wellbore junctions and having commingled fluids with different properties, the mixing method<sup>1</sup> was reviewed. According to this method, an enthalpy balance applied to the mixing of two streams of fluid at different temperatures into one combined stream is used to determine the relative flow rates of those streams.

The development of the equation to calculate the temperature at the mixing point when the two streams are commingled is shown in Appendix A as:

$$T_m = \frac{w_1 C_{p1} T_1 + w_2 C_{p2} T_2}{w_1 C_{p1} + w_2 C_{p2}} \dots \dots \dots (3.5)$$

When the two streams commingling at the junction are the same fluid, so that all heat capacities are the same, combining Eq. 3.5 with the mass balance at the junction

$$w_m = w_1 + w_2 \dots\dots\dots(3.6)$$

can be arranged to yield:

$$\frac{w_1}{w_m} = \frac{T_m - T_2}{T_1 - T_2} \dots\dots\dots(3.7)$$

Thus, if there are measurable temperatures differences between  $T_1$ ,  $T_2$  and  $T_m$ , the fraction of the total flow from each lateral can be determined by measuring these temperatures. This describes the mixing method<sup>1</sup> used for temperature log interpretation.

## CHAPTER IV

### SENSITIVITIES STUDIES AND RESULTS

In this chapter, results of temperature profiles along the build section with different trajectories were calculated. First, the temperature profile for the variable angle trajectory was obtained and compared to a temperature profile with a constant angle of  $45^\circ$ . Additionally, temperature profiles for multilateral wells with two single-phase liquid laterals, and temperature profiles for multilateral wells with two single-phase gas laterals were calculated using the model for single-phase liquid and gas, as well as junction mixing, in order to determine whether the mixing method<sup>1</sup> used in temperature log interpretation could be used to interpret the relative flow rates from different laterals.

#### **4.1 Temperature Profiles along the Build Section with Different Trajectories**

Temperature profiles for several constant angles ( $90^\circ$ ,  $45^\circ$ ,  $25^\circ$ , and  $10.5^\circ$ ) and variable angles along the build section were calculated for an oil flow rate of 3000 STB/D, as shown in Fig. 4.1, using equations 3.1 and 3.2. Table 4.1 summarizes other important characteristics of the reservoir used. As the well deviation from the vertical increases, the temperature at the top of the build section decreases. This is because of the increased length of the wellbore in the build section as the deviation increases, which in turn increases the length of time for the relatively hot wellbore fluid to be cooled by the surrounding formation.

The temperature profile for the variable angle trajectory was surprisingly close to the profile obtained with a constant angle of  $45^\circ$ . Even though these trajectories are quite different (see Figure 4.2), the net heat transfer from the wellbore fluid to the formation was similar.

**Table 4.1 Main Characteristics of the Reservoir - Build Section with Different Trajectories.**

Reservoir characteristic	Values
Geothermal gradient	0.0274 °F/ft
Oil heat capacity	0.485 Btu/lbm°F
Wellbore diameter	7.5 in
Outside casing diameter	5.5 in
Inside casing diameter	5.047 in
Thermal conductivity of cement	96.5 Btu/D ft °F
Thermal conductivity of earth	33.6 Btu/D ft °F
°API	35

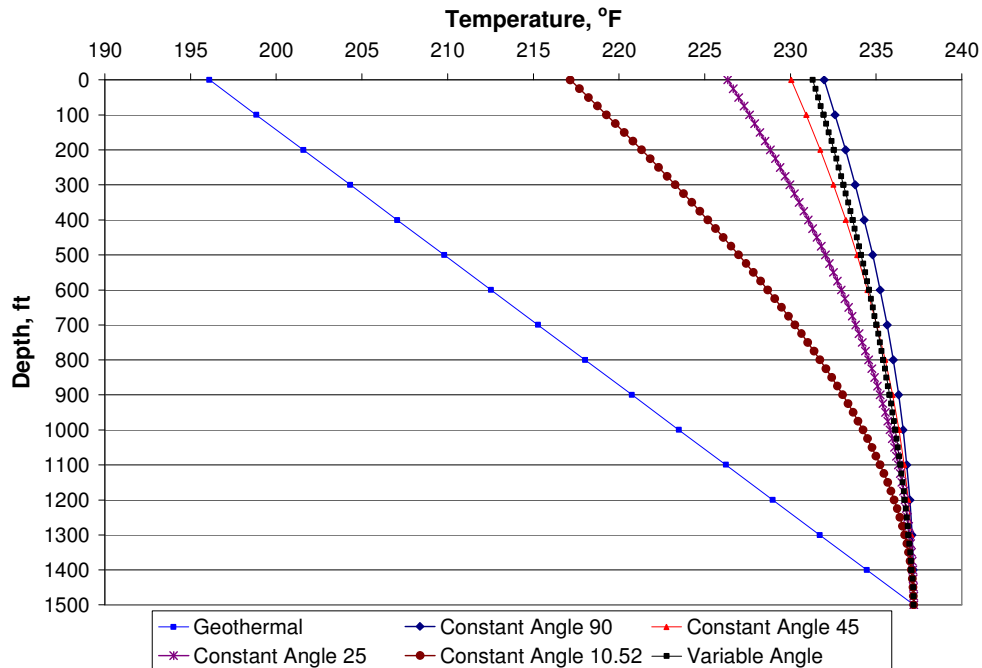


**Fig. 4.1 Temperature profiles along the build section (3000 STB/D).**

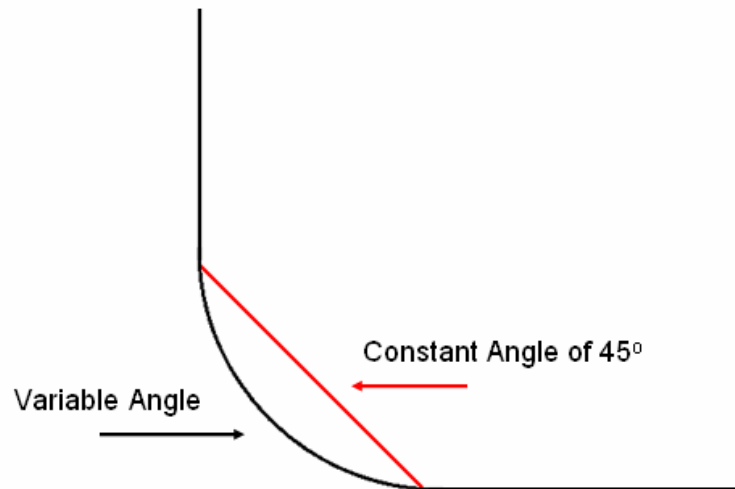


**Fig. 4.2 Constant radius of curvature and constant angle trajectory.**

At a much lower flow rate (200 STB/D), the wellbore cools much more quickly (see Figure 4.3) than at higher flow rate (3000 STB/D), as shown in Figure 4.1, because of the increased length of time for the relatively hot wellbore fluid to be cooled by the surrounding formation.

For the vertical case, the temperature at the top of the build section is less than 10 °F higher than the geothermal temperature; a highly deviated (10.5 °F from the horizontal), constant angle build section has a temperature at the top of the build section that is only 2 °F different from the geothermal temperature.



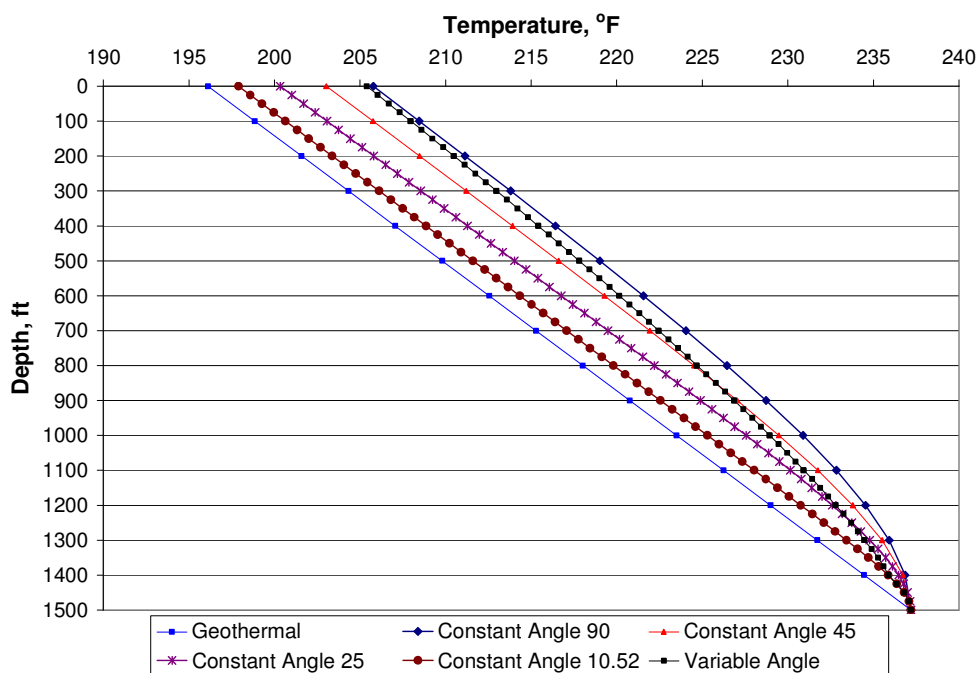


**Fig. 4.3 Temperature profiles along the build section (200 STB/D).**

#### 4.2 Temperature Profiles for Multilaterals: Dual-Lateral with Single-Phase Liquid

Data from Zuata Field in the Orinoco heavy oil belt<sup>10,11</sup> were used to calculate the temperature profiles for multilateral wells with two single-phase liquid laterals, using the model for single-phase liquid and junction mixing. In this area, dual-laterals are expected to achieve a target oil production rate per single well of approximately 3000 STB/D by increasing the contact area between the wellbore and the reservoir. Due to the depth of the reservoir (1500 ft – 2000 ft), the temperatures were moderately low. Down-hole temperature at the total vertical depth was measured to be approximately 120 °F, corresponding to an approximate temperature gradient of 0.02°F/ft, as can be seen in Table 4.2. For the three cases studied, lateral 1 produced 2000 STB/D and lateral 2 produced 3000 STB/D, with an oil gravity of 10° API for both laterals.

To determine whether the mixing method<sup>1</sup> used in the temperature log interpretation could be used to interpret the relative flow rates from different laterals, we simulated

dual laterals produced from different depths as shown in Fig. 4.4. The mixing method depends on the fact that fluids entering a well at different depths have different temperatures due to the geothermal gradient. Similarly, if fluids from two branches of a multilateral have different temperatures before commingling at a junction, the resulting intermediate temperature of the mixed stream should be proportional to the rates from each lateral.

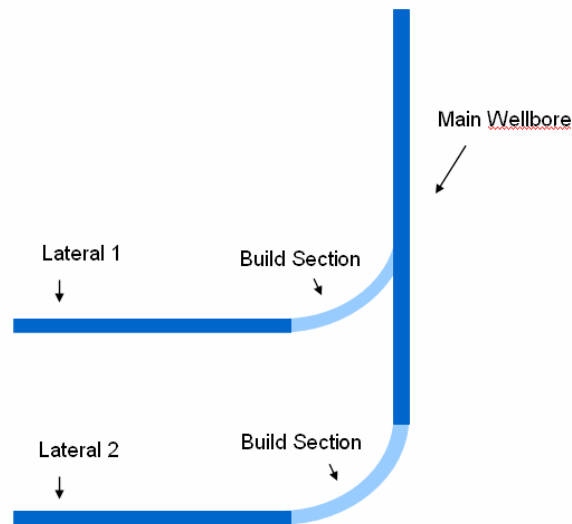


**Fig. 4.4 Dual lateral geometry for examples.**

Figures 4.5 – 4.7 show the predicted temperature profiles for laterals completed at the same depth, laterals completed 500 vertical feet apart, and laterals completed 1000 vertical feet apart. For laterals completed at the same depth (see Figure 4.5), the streams from the two laterals arrive at the junction at slightly different temperatures because of the different flow rates in each lateral. However, the difference is so small (about 0.5 °F) that interpretation of the junction mixing is probably impossible. When the two laterals are spaced at a significant distance (see Figures 4.6 and 4.7), the difference in the temperatures of the fluid from the two laterals is significant enough that the mixing method can be applied. The mixing temperature in these cases is different enough from

the temperature of the lateral (1 °F or more) to be readily measured with current distributed temperature sensor devices.

**Table 4.2 Main Characteristics of the Reservoir - Temperature Profiles for Multilaterals: Dual-Lateral with Single-Phase Liquid.**

Reservoir characteristic	Lateral 1	Lateral 2
Geothermal gradient	0.02 °F/ft	0.02 °F/ft
Oil heat capacity	0.485 Btu/lbm°F	0.485 Btu/lbm°F
Wellbore diameter	7.5 in	7.5 in
Outside casing diameter	5.5 in	5.5 in
Inside casing diameter	5.047 in	5.047 in
Thermal conductivity of cement	96.5 Btu/D ft °F	96.5 Btu/D ft °F
Thermal conductivity of earth	33.6 Btu/D ft °F	33.6 Btu/D ft °F
°API	10	10

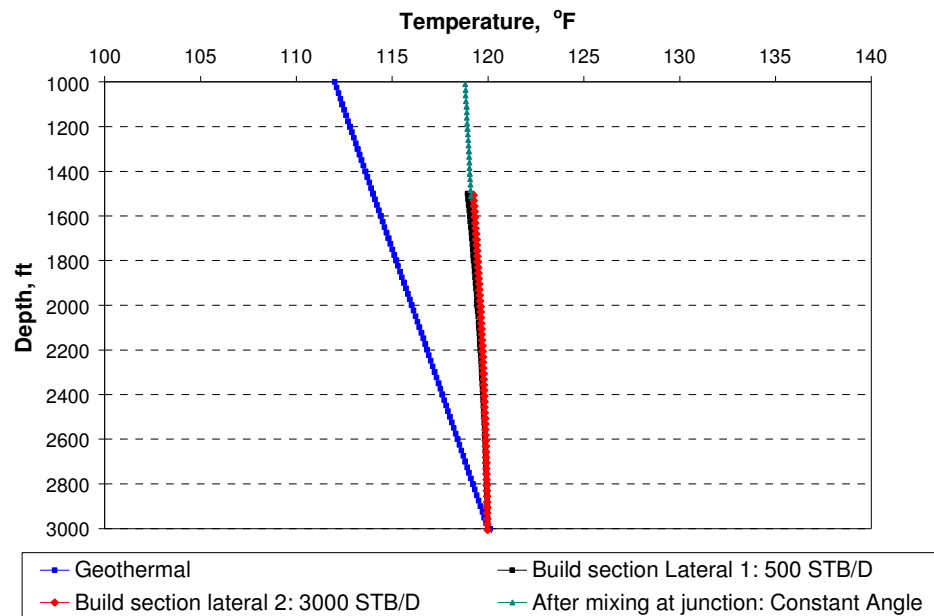


**Fig. 4.5 Build section temperature profiles with liquid production at the same depth.**

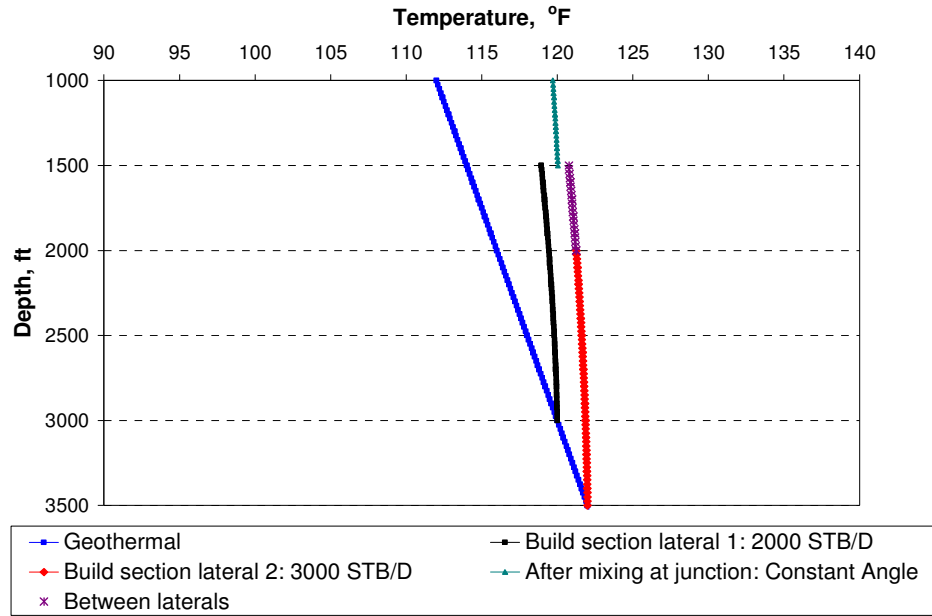


**Fig. 4.6 Build section temperature profiles with liquid production at depths spaced 500 feet apart.**

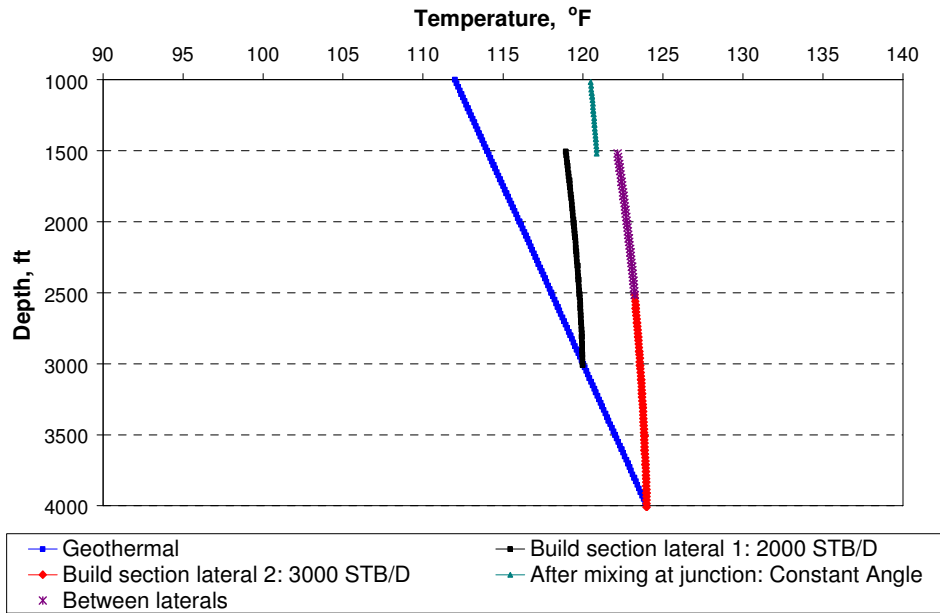


**Fig. 4.7 Build section temperature profiles with liquid production at depths spaced 1000 feet apart.**

When one lateral is producing at a much lower rate than the other, a sizable temperature difference at the junction may occur during production from the same depth at both laterals. Figure 4.8 shows the temperature profiles for production rates of 500 STB/D for lateral 1, and 3000 STB/D for lateral 2, both produced at the same depth. The difference in the temperatures of the streams arriving at the junction is significantly greater than the case with similar rates shown in Figure 4.5.

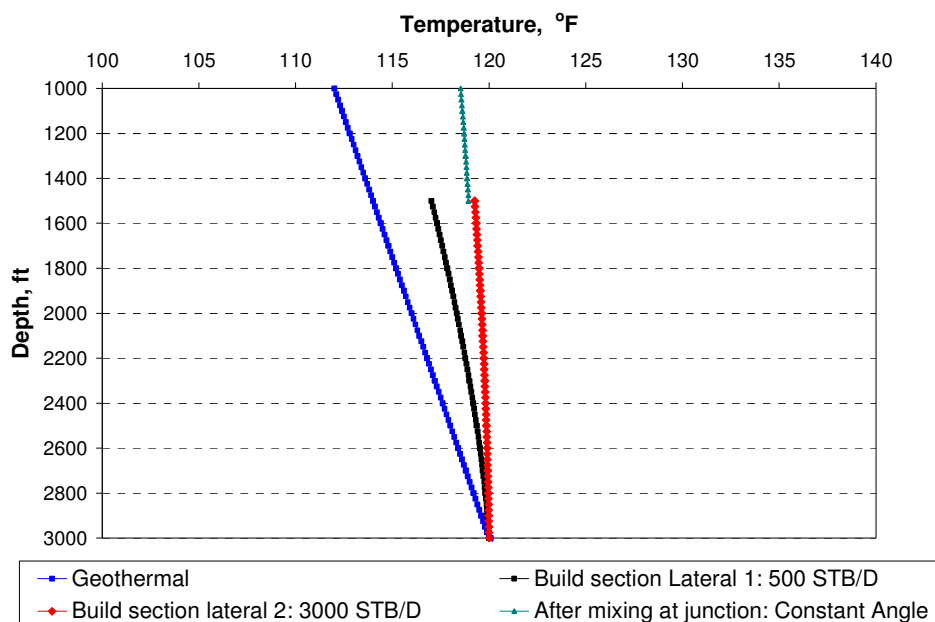


**Fig. 4.8 Build section temperature profiles with different rates of 3000 STB/D and 500 STB/D.**

### 4.3 Cases with Different Fractions of Total Production from Each Lateral: Dual-Lateral with Single-Phase Liquid

Several cases were used for calculations for different fractions of the total production from each lateral, for example if the total production of the well was 5000 STB/D, 20% - 80% means, lateral 1 is producing 1000 STB/D and lateral 2 is producing 4000 STB/D. In these examples, lateral 1 was always kept at the same level, and lateral 2 had a

changing depth (0 ft, 500 ft, and 1000 ft) from lateral 1, and the difference of temperature is calculated at the junction.

The difference in temperature at the junction was calculated in the following fashion: lateral 2 minus lateral 1. Therefore, when the difference is positive it is because lateral 2 has a higher temperature than lateral 1. The total flow rate was kept constant and the fraction flow rate of each lateral changed, and calculations were made for different total flow rates.

When there is a difference in lateral production, we can see that the difference in temperature between the laterals increases as the total flow rate increases, as is illustrated in Figures 4.9 – 4.11, but there is one point when this difference starts decreasing as the flow rate increases. All the differences in depth between the laterals are 0 ft, 500 ft and 1000 ft. This is due to the fact that after certain flow rates (especially high flow rates), the lateral which is producing less increases temperature in a more rapid manner than the lateral which is producing more. This effect is delayed when there is a difference in depth between the laterals. Even though lateral 1 increases rapidly temperature, lateral 2 also increases because it is deeper than lateral 1. However, eventually the difference in temperature will decrease, even for very high flow rate. For very high flow rate the difference in temperature between the laterals at the junction would have a small value, but for those cases where there is a difference in depth, the resulting effect would be delayed.

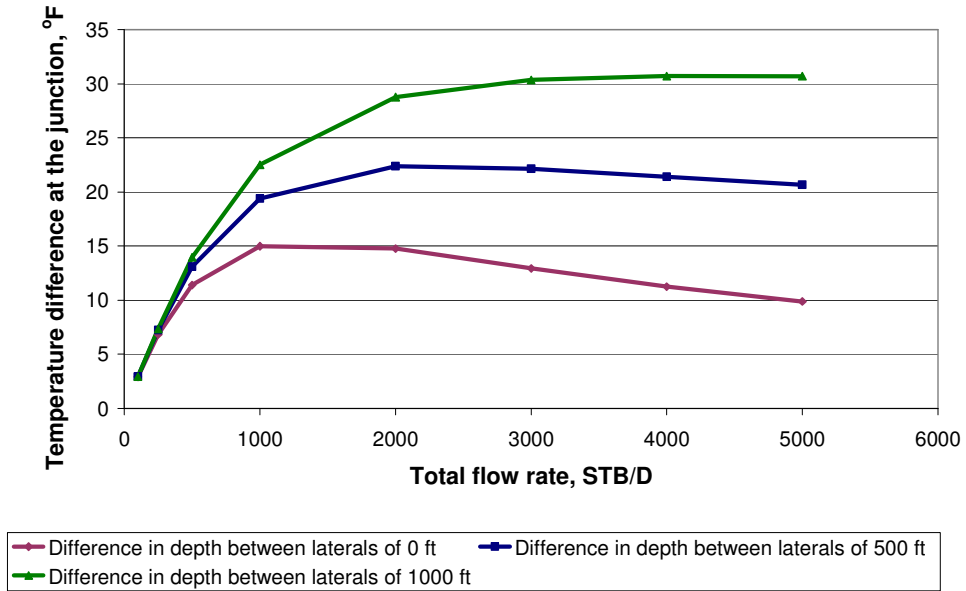


**Fig. 4.9 Fraction of total production from each lateral: 20% - 80%.**

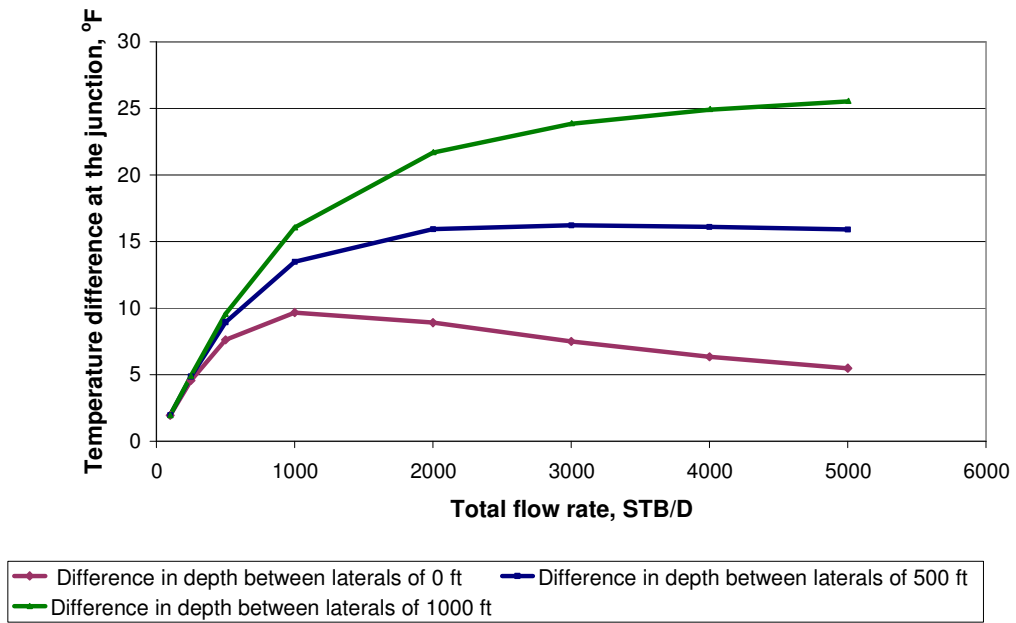


**Fig. 4.10 Fraction of total production from each lateral: 30% - 70%.**

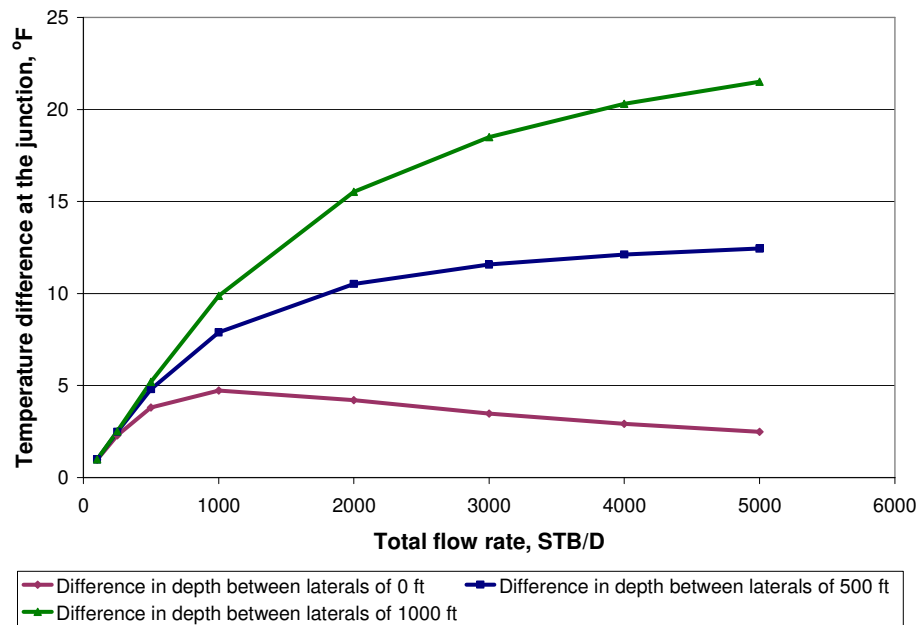


**Fig. 4.11 Fraction of total production from each lateral:  
40% - 60%.**

When the two laterals produce the same flow rate and are at the same level, there is not difference in temperatures at the junction. Therefore, the mixing method can not be applied (as can be seen in Figure 4-12). The mixing method can be applied when there is a difference in depth between the laterals, and the total flow rate is large enough to have an appreciable temperature difference at the junction measurable by a sensor.



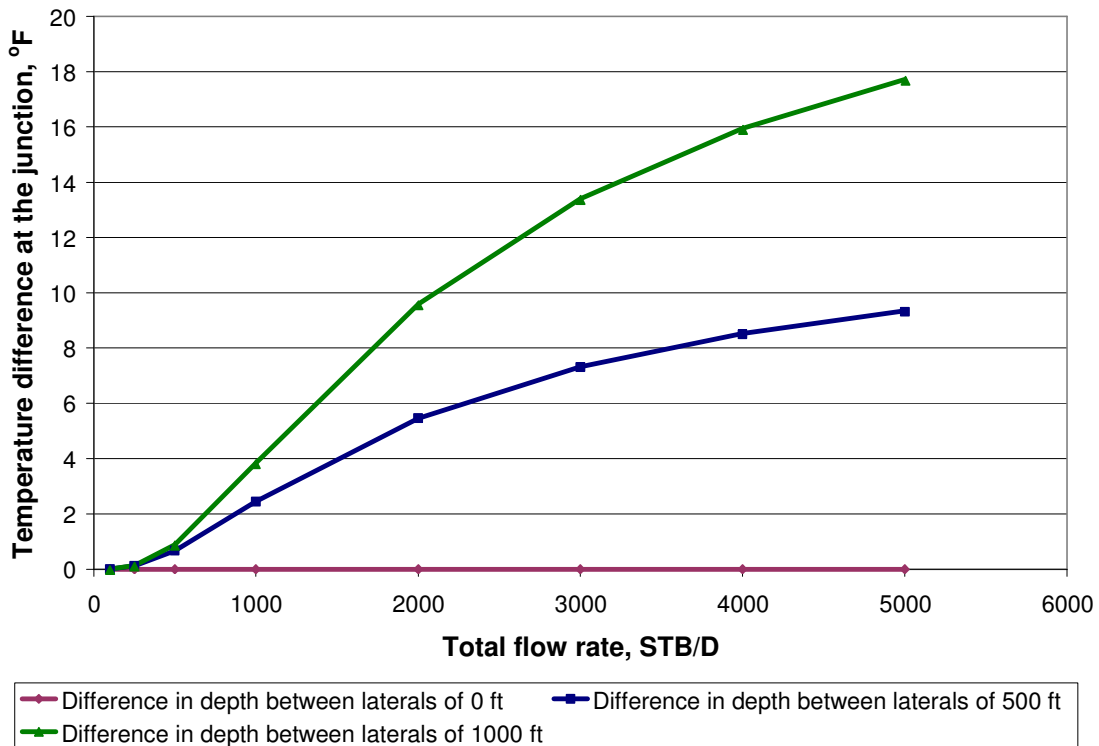


**Fig. 4.12 Fraction of total production from each lateral: 50% - 50%.**

When a lateral which is producing more is kept at the same level while the other lateral which is producing less is moved to changing depths, there is one instant when there is no difference in temperature at the junction (as shown in Figures 4.13 - 4.15). This level is reached when the effect of having a high flow rate from lateral 1 has the same effect as having a difference in depth from lateral 2, which has a lower flow rate. If the laterals have a significant difference in flow rate, this effect will not be visible.

From Figures 4.13 – 4.15 we see that the absolute difference in temperature at the junction for different total flow rates can be seen to be smaller for all cases, because the effect of having a higher flow rate is larger than having depth differences between the laterals. Also, in this case lateral 1 will always have a higher temperature than lateral 2, because of its higher flow rate. However, when the total flow rate increases, there is a point where lateral 2 has a higher temperature than lateral 1.

When there is a difference in the lateral's production, it can be seen that the difference in temperature between the laterals usually decreases as the total flow rate increases. However, there is one point where this difference begins to increase as the flow rate increases for all the differences in depth. These differences between the laterals are 0 feet, 500 feet and 1000 feet as shown in Figures 4.13 – 4.15. This is due to the fact that above certain flow rates (high flow rates), the lateral producing less increases in temperature in a more rapidly manner than the lateral producing more. When there is a difference in depth between the laterals, the lateral which has less production but a changing depth will increase in temperature even more rapidly than if the laterals are at the same level. Also, when both laterals are at the same level, the difference in temperature decreases for high flow rates. Therefore, for high flow rates and laterals at the same level, the difference in temperature at the junction has a low value.

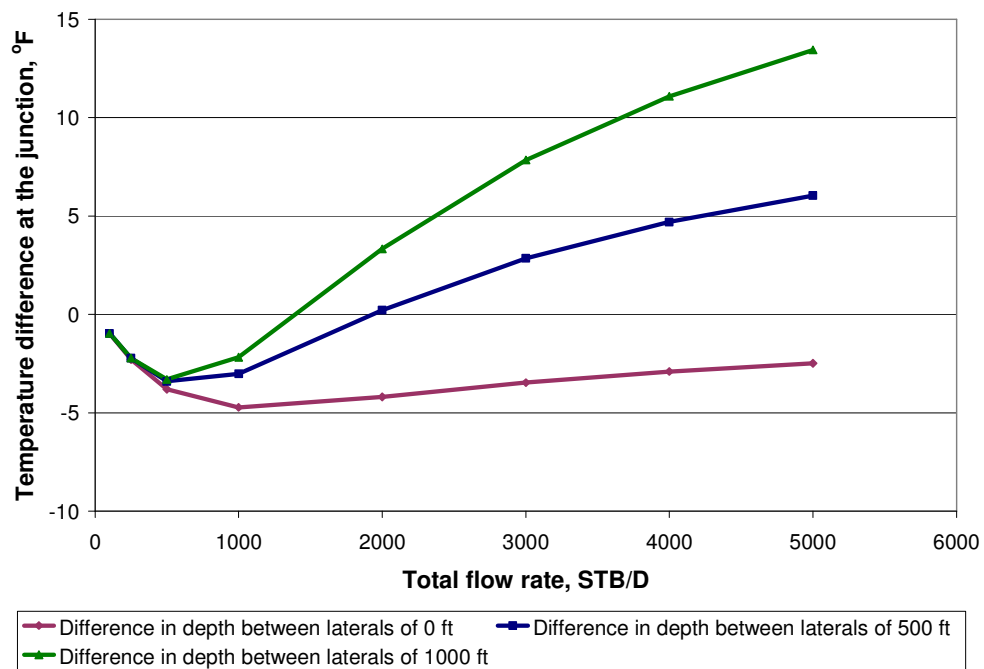


**Fig. 4.13 Fraction of total production from each lateral: 60% - 40%.**

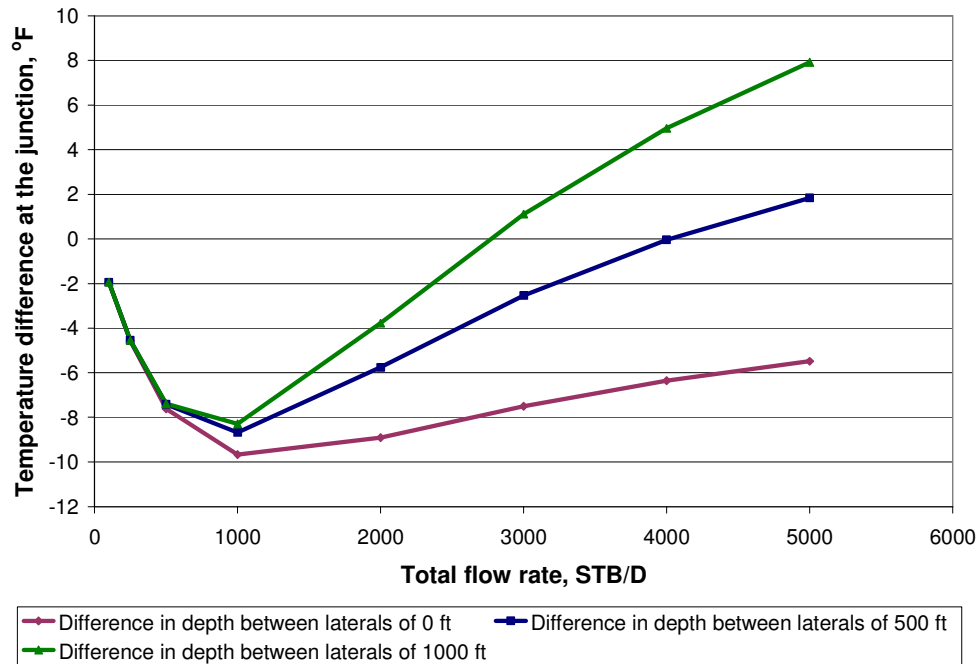


**Fig. 4.14 Fraction of total production from each lateral: 70% - 30%.**

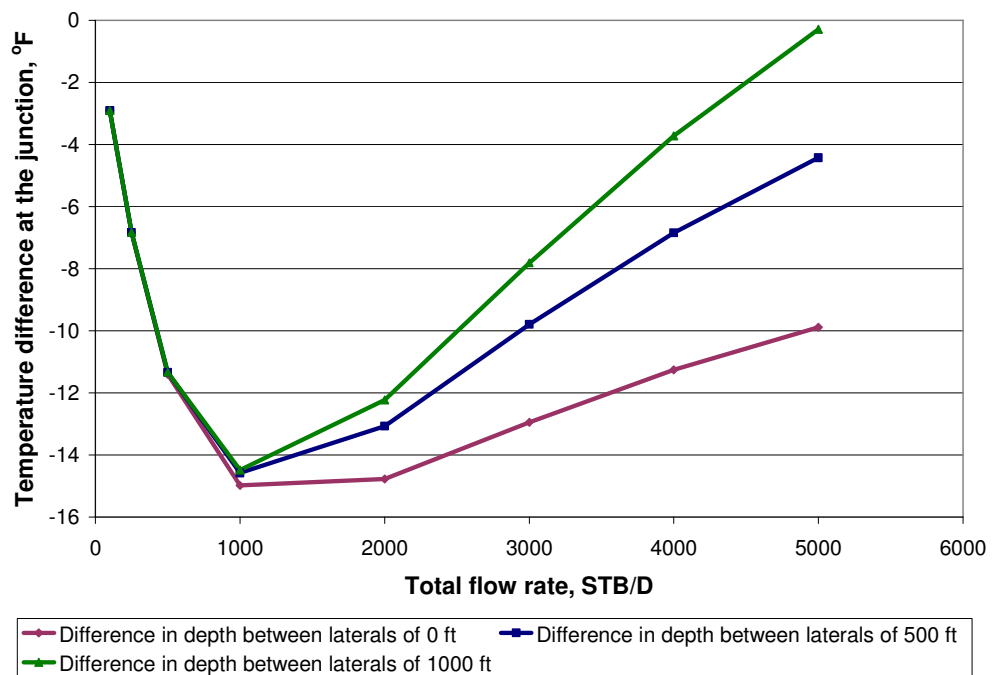


**Fig. 4.15 Fraction of total production from each lateral: 80% - 20%.**

#### 4.4 Temperature Profiles for Multilaterals: Dual-Lateral with Single-Phase Gas

Typical data from the Parks Field Unit in west Texas<sup>12</sup> shown in Table 4.3 were used to calculate the temperature profiles for multilateral wells with two single-phase gas laterals, using the model for single-phase gas in the build section and mixing at the junction. Wells are design to produce gas from the upper and lower porosity lenses of geologically constrained Devonian limestone. The results from temperature profiles for this case are shown in Figures 4.16 – 4.18, where lateral 1 produces 700 Mscf/D and lateral 2 produces 1.7 MMscf/D. The geothermal temperature gradient used was 0.016°F/ ft.

**Table 4.3 Main Characteristics of the Reservoir - Temperature Profiles for Multilaterals: Dual-Lateral with Single-Phase Gas.**

<b>Reservoir characteristic</b>	<b>Lateral 1</b>	<b>Lateral 2</b>
Geothermal gradient	0.016 °F/ft	0.016 °F/ft
Oil heat capacity	0.3 Btu/lbm°F	0.3 Btu/lbm°F
Wellbore diameter	7.5 in	7.5 in
Outside casing diameter	5.5 in	5.5 in
Inside casing diameter	5.047 in	5.047 in
Thermal conductivity of cement	96.5 Btu/D ft °F	96.5 Btu/D ft °F
Thermal conductivity of earth	33.6 Btu/D ft °F	33.6 Btu/D ft °F
Gas gravity	1.04	1.04

The results for these gas production cases are similar to those for an oil producing dual lateral. The larger the vertical separation between the laterals, the bigger the temperature difference between the produced streams arriving at the junction. For a vertical spacing of 500 or 1000 feet, the temperature difference between the streams is easily discernible, allowing the application of the mixing method to interpret the relative flow rates from the laterals.

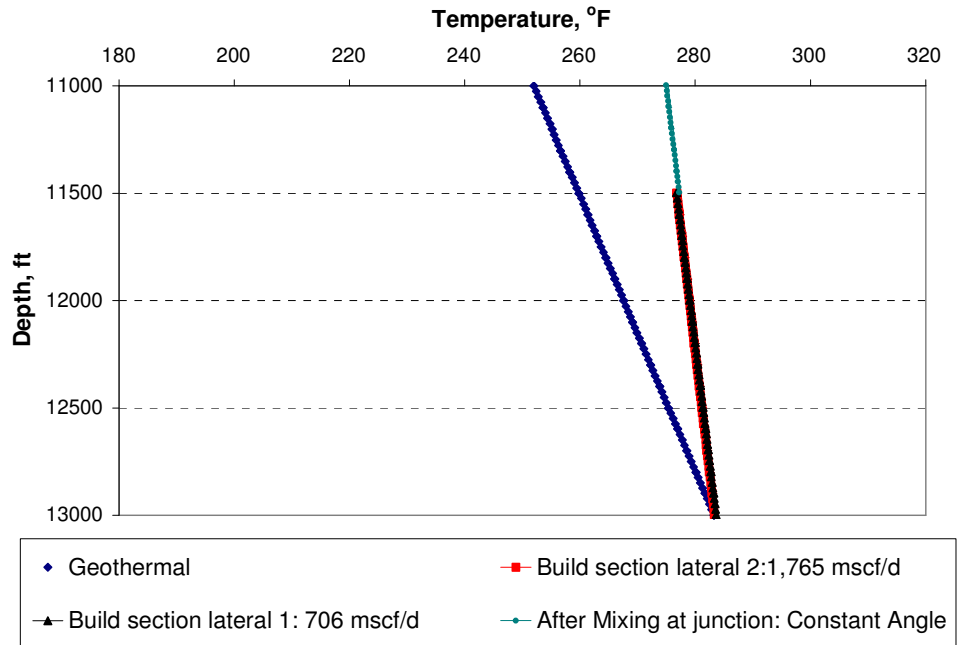


**Fig. 4.16 Build section temperature profiles with gas production at the same depth.**

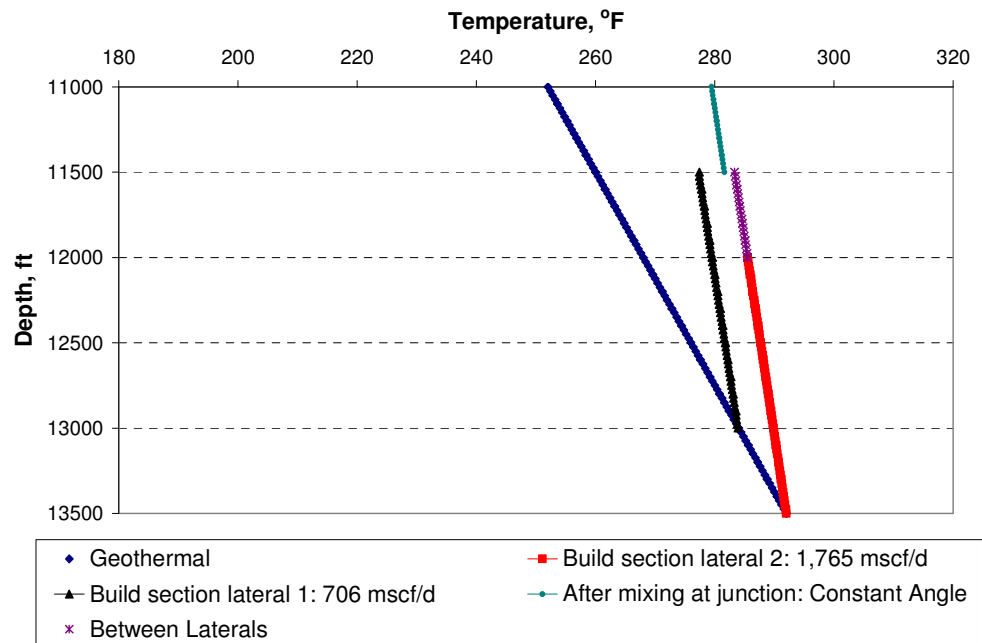


**Fig. 4.17 Build section temperature profiles with gas production at depths spaced 500 feet apart.**

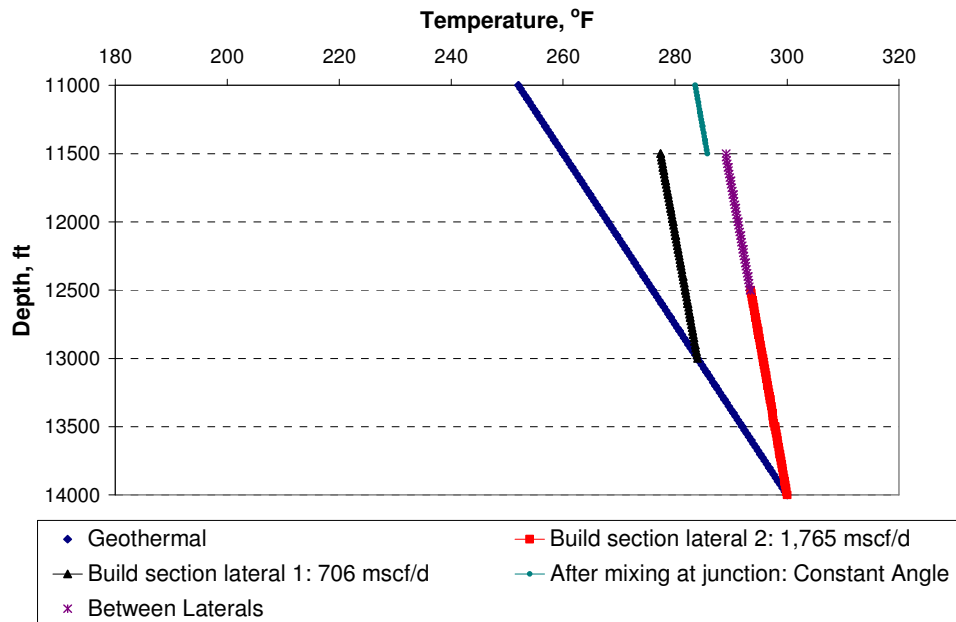


**Fig. 4.18 Build section temperature profiles with gas production at depths spaced 1000 feet apart.**

#### 4.5 Summary

Based on the results and sensitivities cases studied, several interesting observations follow: 1) when we consider the effect of variable angles on the build section, we were able to calculate different temperature profiles for variable angles and different constant angles in order to compare the effects. 2) From the model for single-phase liquid and gas and junction mixing, the temperature profiles for multilateral wells with two single-phase liquid laterals and two single-phase gases were analyzed in this research. As a result, we were able to obtain different temperature profiles for different depths and flow rates between the laterals. This means that the effect of different depths and flow rates are significant and need to be taken into account.

Also, these results helped to determine whether the mixing method<sup>1</sup> used in temperature log interpretation could also be used to interpret the relative flow rates from different laterals.

## CHAPTER V

### CONCLUSIONS

We have developed a model to predict temperature profiles in the variable angle build sections of a multilateral well by applying the method developed by Ramey to this geometry. In addition, we have applied an energy balance to a multilateral junction where two flow streams are commingled. From these models of temperature behavior in multilaterals we find:

1. The temperature of the fluids produced from two laterals will differ significantly at the junction when the streams are commingled, if the laterals are producing from reservoirs at different depths. This is because the fluids produced have different temperatures, due to the geothermal gradient.
2. A significant temperature difference between the two streams can also occur when the flow rates from the two laterals differ greatly.
3. When measurable differences between the temperatures just below a junction occur, the mixing method of production log interpretation can be used to estimate the fraction of flow produced from each lateral.



## NOMENCLATURE

$A$	=	inverse relaxation parameter, ft
$C_p$	=	specific heat capacity, BTU/lb <sub>m</sub> °F
$C_j$	=	Joule-Thomson coefficient, °F/psi
$C_I$	=	integration constant
$D$	=	length of a discrete segment of build section, ft
$f(t)$	=	time function, dimensionless
$g$	=	acceleration of gravity, 32.2 ft/s <sup>2</sup>
$g_c$	=	conversion factor, 32.17 lbm-ft/lbf-s <sup>2</sup>
$g_G$	=	geothermal gradient, °F/ft
$H$	=	enthalpy per unit mass, BTU/lb <sub>m</sub>
$J$	=	mechanical equivalent of heat, 778 ft-lb <sub>f</sub> /BTU
$k_{cem}$	=	conductivity of cement, Btu/hr-ft- °F
$k_e$	=	conductivity of earth or formation, Btu/hr-ft- °F
$L$	=	total measure of well depth, ft
$p$	=	pressure, psi
$Q$	=	heat transfer rate per unit length of wellbore, Btu/hr-ft
$R$	=	constant radius between the main wellbore and horizontal lateral,ft
$r$	=	radius, ft
$t$	=	production time, hr
$T$	=	temperature, °F
$T_G$	=	formation temperature at any radial distance, °F
$T_{Gi}$	=	formation temperature at initial condition, °F
$T_{Gibh}$	=	static formation temperature at the bottom hole, °F
$T_f$	=	fluid temperature, °F
$T_{f(known)}$	=	last fluid temperature of final segment, °F
$T_m$	=	mixed stream temperature, °F
$U$	=	overall heat transfer coefficient, Btu/hr-ft <sup>2</sup> - °F
$v$	=	fluid velocity, ft/s
$V$	=	specific volume
$w$	=	mass flow rate of fluid, lbm/s
$X$	=	horizontal length of each discrete segment, ft
$z$	=	variable well depth from surface, ft
$\alpha$	=	wellbore inclination with horizontal, degrees
$\gamma, \lambda$	=	angles between horizontals of each discrete segment, ft
$\rho$	=	density, lb <sub>m</sub> /ft <sup>3</sup>
$\sigma$	=	thermal diffusivity, ft <sup>2</sup> /sec

**Subscripts**

<i>ci</i>	=	casing inside
<i>co</i>	=	casing outside
<i>m</i>	=	mixed stream
<i>to</i>	=	tubing outside
<i>wb</i>	=	wellbore
1	=	stream 1
2	=	stream 2

## REFERENCES

1. Hill, A.D.: *Production Logging-Theoretical and Interpretive Elements*, Monograph Series SPE, Richardson, TX (1990) **14**, 28.
2. Ramey, H.J., Jr.: *Wellbore Heat Transmission*, Journal of Petroleum Technology, *Trans. AIME* (1962) **225**, 427.
3. Carslaw, H.S. and Jaeger, J.C.: *Conduction of Heat in Solids*, Oxford U. Press, Amen House, London (1950).
4. Chen, W., Zhu, D., and Hill, A.D.: *A Comprehensive Model of Multilateral Well Deliverability*, paper SPE 64751 presented at the 2000 SPE International Oil and Gas Conference and Exhibition in China held in Beijing, China, 7-10 November.
5. Joshi, S.D.: *Augmentation of Well Productivity with Slant and Horizontal Wells*, Journal of Petroleum Technology (June 1988), 729.
6. Babu, D.K., and Odeh A.S.: *Productivity of a Horizontal Well*, SPE Reservoir Engineering (November 1989), 417.
7. Sagar, R.K., Dotty, D.R., and Schmidt, Z.: *Predicting Temperature Profiles in a Flowing Well*, SPEPE (November 1991), 441.
8. Hasan, A.R. and Kabir, C.S.: *Aspects of Wellbore Heat Transfer During Two-Phase Flow*, SPEPE (August 1994), 211.
9. Hasan, A.R. and Kabir, C.S.: *Fluid Flow and Heat Transfer in Wellbores*, Society of Petroleum Engineers, Richardson, TX (2002).
10. Ramirez, R., Fernandez, V., and Barrios J.: *Multilateral Field Experience in Developing an Extra Heavy Crude-Oil Reservoir*, paper SPE 86947 presented at the

2004 SPE International Thermal Operations and Heavy Oil Symposium and Western Regional Meeting held in Bakersfield, CA, USA, 16-18 March.

11. Robles, Jorge: *Application of Advanced Heavy-Oil-Production Technologies in the Orinoco Heavy-Oil-Belt, Venezuela*, paper SPE 69848 presented at the 2001 International Thermal Operations and Heavy Oil Symposium held in Margarita Island, Venezuela, 12-14 March.
12. Owodunni, A., Travis, T., and Dunk, G.: *The Use of Multilateral Technology to Arrest Production Decline in a West-Texas Gas Field*, paper SPE 84029 presented at the 2003 SPE Annual Technical Conference and Exhibition held in Denver, Colorado, USA, 5-8 October.

## APPENDIX A

### DERIVATION OF FLUID TEMPERATURE MODELS

In this appendix, we derive equations describing the temperature in a variable angle build section and at a well junction, when two streams mix.

#### Build Section

To determine the temperature profile of a build section where the well inclination is changing, we extended Ramey's<sup>2</sup> method to this flow geometry, as follows:

Applying an energy balance for a segment along the build section as a control volume as shown in Figure A-1, yields

$$\frac{dH}{dz} + \frac{g \sin \alpha}{g_c J} + \frac{v}{g_c J} \frac{dv}{dz} = \pm \frac{Q}{w} \dots\dots\dots(A-1)$$

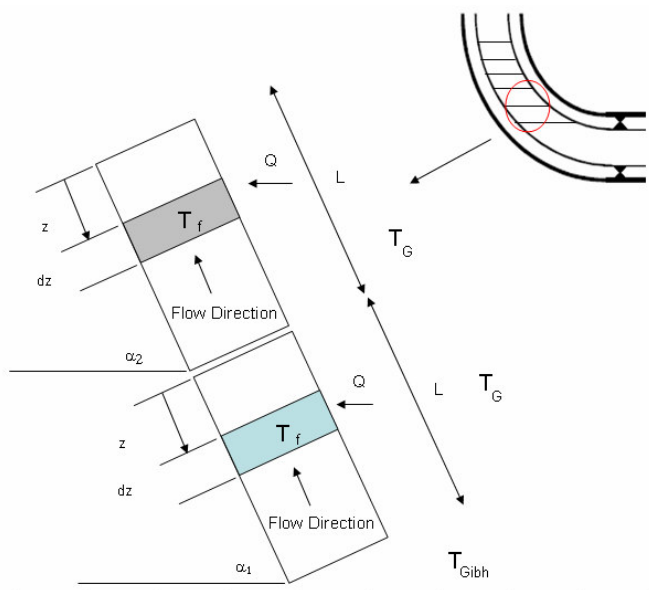


**Fig. A-1 Control volume**

The enthalpy is defined by

$$dH = C_p dT_f - C_j C_p dp \dots\dots\dots(A-2)$$

By substituting equation (A-2) into (A-1), we get

$$\frac{dT_f}{dz} = C_j \frac{dp}{dz} + \frac{1}{C_p} \left[ \frac{Q}{w} - \frac{g \sin \alpha}{Jg_c} - \frac{v}{Jg_c} \frac{dv}{dz} \right] \dots\dots\dots(A-3)$$

The heat flow through the completion can be represented as

$$Q = -2\pi r_{io} U_{io} (T_f - T_{wb}) \dots\dots\dots(A-4)$$

and the heat loss to the formation as

$$Q \equiv -\frac{2\pi k_e}{f(t)} (T_{wb} - T_{Gi}) \dots\dots\dots(A-5)$$

Combining equations (A-4) and (A-5) yields

$$Q \equiv -\frac{wC_p}{A} (T_f - T_{Gi}) \dots\dots\dots(A-6)$$

where A is defined as

$$A = \left( \left( \frac{2\pi}{wC_p} \right) \left[ \frac{r_{ci} U k_e}{k_e + r_{ci} U f(t)/12} \right] \frac{1}{86400 \times 12} \right)^{-1} \dots\dots\dots(A-7)$$

Substituting equation (A-6) into (A-3), the equation becomes (A-8):

$$\frac{dT_f}{dz} = \frac{(T_f - T_{Gi})}{A} - \frac{g \sin \alpha}{C_p Jg_c} - \frac{v}{C_p Jg_c} \frac{dv}{dz} + C_j \frac{dp}{dz} \dots\dots\dots(A-8)$$

### *Single-Phase Liquid*

The following assumptions were made in order to develop the equation for single-phase liquid: incompressible fluids; kinetic energy becomes negligible; flowing friction becomes negligible, radiation and convection coefficients are negligible and can be ignored for the calculation of overall heat transfer. Also, because steel has a high thermal conductivity, the thermal resistance of the pipe and casing are negligible as compared to the thermal resistance of the material in the casing.

For single phase liquid flow, the static head loss nearly equals the total pressure gradient.

$$\frac{dp}{dz} = \rho \left( \frac{g}{g_c} \right) \sin \alpha \dots\dots\dots(A-9)$$

Liquid density variation with pressure is usually very small, so the Joule-Thomson coefficient can be defined as

$$C_j \equiv \frac{1}{C_p} \left[ \frac{\partial H}{\partial p} \right]_T = \frac{V}{C_p} = \frac{1}{\rho C_p} \dots\dots\dots(A-10)$$

and the final energy balance becomes

$$\frac{dT_f}{dz} = \pm \frac{(T_f - T_{Gi})}{A} \dots\dots\dots(A-11)$$

where

$$T_{Gi} = T_{Gibh} - (L - z)g_G \sin \alpha \dots\dots\dots(A-12)$$

Substituting equation (A-12) into (A-11), the equation becomes

$$\frac{dT_f}{dz} = \frac{1}{A} \{ T_f - [T_{Gibh} - (L - z)g_G \sin \alpha] \} \dots\dots\dots(A-13)$$

Solving the first-order linear differential equation with the integration factor method yields

$$T_f = T_{Gi} + Ag_G \sin \alpha + C_1 \exp\left(\frac{z-L}{A}\right) \dots\dots\dots(A-14)$$

$$T_f = T_{Gibh} - (L-z)g_G \sin \alpha + Ag_G \sin \alpha + C_1 \exp\left(\frac{z-L}{A}\right) \dots\dots\dots(A-15)$$

### *Boundary Conditions for Single-Phase Liquid*

For fluid coming from the formation at the bottom hole location ( $z=L$ ) fluid temperature and geothermal temperature are the same ( $T_f = T_{Gibh}$ ). The integration constant for this boundary condition yields

$$C_1 = -Ag_G \sin \alpha \dots\dots\dots(A-16)$$

Substituting equation (A-16) into (A-15), the equation becomes

$$T_f = T_{Gibh} - g_G \sin \alpha \left[ (L-z) - \left( 1 - \exp\left(\frac{z-L}{A}\right) \right) A \right] \dots\dots\dots(A-17)$$

For other segments, the initial fluid temperature is equal to the last fluid temperature of the last segment.

$$C_1 = T_f(\text{known}) - T_{Gi} - Ag_G \sin \alpha \dots\dots\dots(A-18)$$

$$T_f = T_{Gi} + Ag_G \sin \alpha + [T_f(\text{known}) - T_{Gi} - Ag_G \sin \alpha] \exp\left(\frac{z-L}{A}\right) \dots\dots\dots(A-19)$$



### *Single-Phase Gas*

In the case of single-phase gas the static head loss is not the same as the total pressure gradient, but these two terms together can be neglected for gases a low pressure. Solving the equation (A-8) yields

$$T_f = T_{Gi} + A \left( g_G \sin \alpha - \frac{g \sin \alpha}{C_p J g_c} \right) + C_I \exp[(z-L)/A] \dots\dots\dots(A-20)$$

### *Boundary Conditions for Single-Phase Gas*

For the first segment where fluid is coming from the formation at the bottom of the hole ( $z=L$ ), the fluid temperature and the geothermal temperature are the same ( $T_f = T_{Gibh}$ ). The integration constant for this boundary condition is

$$C_I = -A \left( g_G \sin \alpha - \frac{g \sin \alpha}{C_p J g_c} \right) \dots\dots\dots(A-21)$$

Substituting equation (A-21) into (A-20), the equation becomes

$$T_f = T_{Gibh} + \left\{ A - A \left[ \exp((z-L)/A) \right] \right\} \left( g_G \sin \alpha - \frac{g \sin \alpha}{C_p J g_c} \right) \dots\dots\dots(A-22)$$

For other segments, the initial fluid temperature is equal to the last fluid temperature of the last segment.

$$C_I = T_{f \text{ known}} - T_{Gi} + A \left( g_G \sin \alpha - \frac{g \sin \alpha}{C_p J g_c} \right) \dots\dots\dots(A-23)$$

$$T_f = T_{Gi} + A \left( g_G \sin \alpha - \frac{g \sin \alpha}{C_p J g_c} \right) + \exp[(z-L)/A] \left\{ T_{f \text{ known}} - T_{Gi} + A \left( g_G \sin \alpha - \frac{g \sin \alpha}{C_p J g_c} \right) \right\} \dots\dots\dots(A-24)$$

### ***Overall Heat Transfer Coefficient for Casing Flow***

The radiation and convection coefficients are negligible and can be ignored for the calculation of overall heat transfer. Also, because steel has a high thermal conductivity, the thermal resistance of the casing is negligible as compared to the thermal resistance of the casing, so the heat transfer coefficient is

$$U = \frac{12}{r_{ci}} \left[ \frac{\ln(r_{wb} / r_{co})}{k_{cem}} \right]^{-1} \dots\dots\dots(A-25)$$

### ***Time Function $f(t)$ .***

Ramey<sup>2</sup> presented procedures for finding the function  $f(t)$ . For extended periods of time, it can be approximated by

$$f(t) = -\ln \frac{r_{co}}{2\sqrt{\sigma t}} - 0.290 \dots\dots\dots(A-26)$$

### **Wellbore Junction (Mixing Point)**

Applying an energy balance to the wellbore junction system, considering no heat loss and gain during the mixing process, yields

$$w_1 C_{p1} (T_m - T_1) + w_2 C_{p2} (T_m - T_2) = 0 \dots\dots\dots(A-27)$$

And the temperature of a mixture can be defined by

$$T_m = \frac{w_1 C_{p1} T_1 + w_2 C_{p2} T_2}{w_1 C_{p1} + w_2 C_{p2}} \dots\dots\dots(A-28)$$

The following equation was used to calculate the heat capacity of a mixture:

$$C_{pm} = \left( \frac{w_1}{w_1 + w_2} \right) C_{p1} + \left( \frac{w_2}{w_1 + w_2} \right) C_{p2} \dots\dots\dots (A-29)$$

## APPENDIX B

### GEOMETRY OF THE BUILD SECTION

The build section geometry was calculated assuming a constant radius of curvature between the horizontal wellbore and the main wellbore by a number of discrete wellbore increments of same the length, each having a constant angle. As a result, the build section presents variable inclination geometry, as shown in Figure B-1. Other trajectories can be handled in a similar manner to the one presented here.

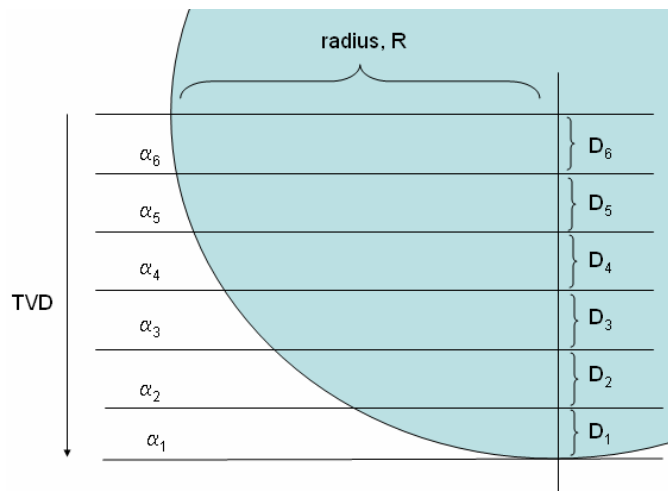


**Fig. B-1 Geometry of Build Section**

#### *Angle from Each Segment*

For the first discrete segment, in order to calculate the length of segment  $X_1$ , the angle  $\beta$  was calculated using the equations B-1 and B-2 from trigonometric definitions, as shown in Figure B-2.

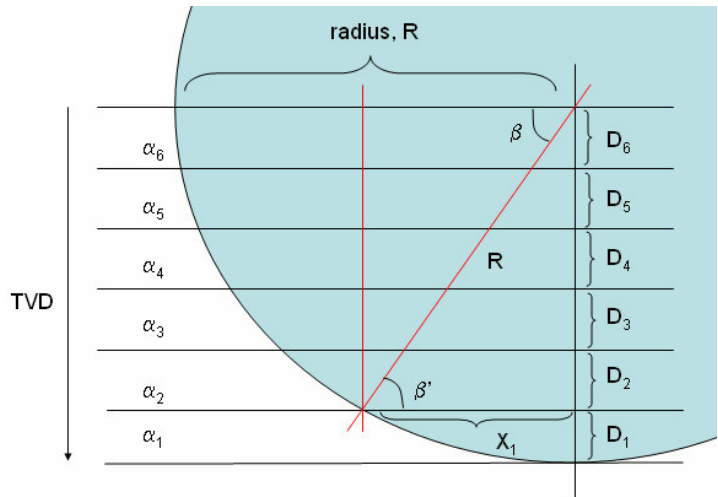


**Fig. B-2 Demonstration of how to calculate segment  $X_1$**

$$\sin(\beta) = \frac{D_6 + D_5 + D_4 + D_3 + D_2}{R} \dots\dots\dots(B-1)$$

$$\beta = \arcsin\left(\frac{D_6 + D_5 + D_4 + D_3 + D_2}{R}\right) \dots\dots\dots(B-2)$$

Also, angles  $\beta$  and  $\beta'$  are the same as that which is shown in Figure B-2,

$$\beta = \beta' \dots\dots\dots(B-3)$$

So, the length of  $X_1$  can be approximated by

$$X_1 = \cos(\beta') \times R \dots\dots\dots(B-4)$$

After calculating the length of segment  $X_1$ , the calculations necessary to obtain the angle  $\gamma$  are based on knowing both lengths  $X_1$  and  $D_1$ , and on using the definition of a tangent as follows (and is illustrated in Figure B-3):

$$\tan(\gamma) = \frac{D_1}{X_1} \dots\dots\dots(B-5)$$

$$\gamma = \arctan\left(\frac{D_1}{X_1}\right) \dots\dots\dots(B-6)$$

Knowing that the sum of the angles inside a triangle must be 180 degrees, and also knowing the value of two of the three angles ( $\gamma$  and 90 degrees), the angle  $\lambda$  can be calculated as follows:

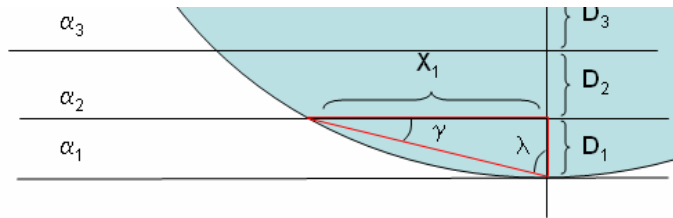


**Fig. B-3 Demonstration of how to calculate the angle  $\gamma$**

$$\lambda = 180 - (\gamma + 90) \dots\dots\dots(B-7)$$

Yielding the solution for  $\alpha_1$  as

$$\alpha_1 = 90 - \lambda \dots\dots\dots(B-8)$$

For other discrete segments, the procedure to determine the length of segment  $X_2$  is the same as the one used to calculate the length of segment  $X_1$ , but because the model was developed beginning with the lowest segment connected to a horizontal lateral, one of the distances of the triangle gets smaller as we move up. This can be seen in Figure B-4. Also, the procedure is repeated in order to calculate the other lengths,  $X_3$ ,  $X_4$ , etc. until we get to the last segment.

$$\sin(\beta) = \frac{D_6 + D_5 + D_4 + D_3}{R} \dots\dots\dots(B-9)$$

$$\beta = \arcsin\left(\frac{D_6 + D_5 + D_4 + D_3}{R}\right) \dots\dots\dots(B-10)$$

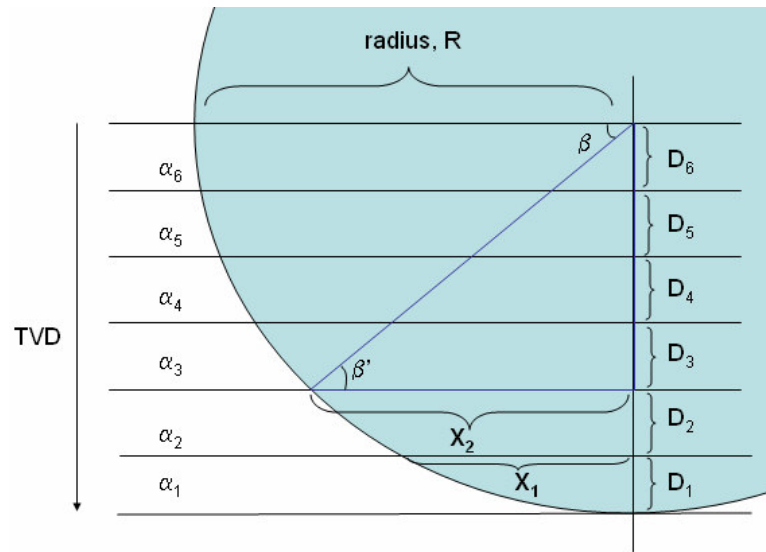


**Fig. B-4 Demonstration of how to calculate segment X<sub>2</sub>**

Also, angles \$\beta\$ and \$\beta'\$ are the same, as shown in Figure B-4.

$$\beta = \beta' \dots\dots\dots(B-11)$$

So, the length of \$X\_2\$ can be approximated by

$$X_2 = \cos(\beta') \times R \dots\dots\dots(B-12)$$

After calculating the length of segment  $X_2$ , the calculations to obtain the angle  $\tau_1$  are based on knowing both lengths  $(X_2 - X_1)$  and  $D_2$ , and using the definition of a tangent as follows (and is illustrated in Figure B-5):

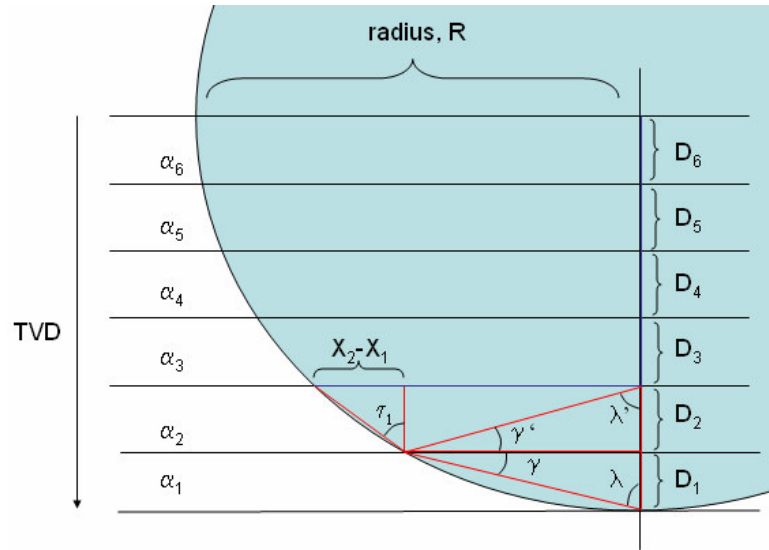


**Fig. B-5 Demonstration of how to calculate the angle  $\tau_1$**

$$\tan(\tau_1) = \frac{X_2 - X_1}{D_2} \dots\dots\dots(B-13)$$

$$\tau_1 = \arctan\left(\frac{X_2 - X_1}{D_2}\right) \dots\dots\dots(B-14)$$

Yielding the solution for  $\alpha_2$  as,

$$\alpha_2 = (90 - \tau_1) \dots\dots\dots(B-15)$$

This procedure was repeated for all discrete segments until we reached the final segment.



**VITA**

Name: Analis Romero Lugo

Permanent Address: Av. 11 B # 49B-51, Urb. Canta Claro  
Maracaibo, Edo. Zulia  
Venezuela

Email: analis\_romero@yahoo.com

Education: B. S., Chemical Engineering,  
Universidad del Zulia, Maracaibo,  
Venezuela  
(May 1996)

M.S., Petroleum Engineering  
Texas A&M University  
College Station, TX 77843-3116, USA  
(August 2005)